Scientific Journals
Maritime University of Szczecin

Zeszyty Naukowe
Akademia Morska w Szczecinie

2009, 18(90) pp. 83–88

2009, 18(90) s. 83–88

Detection of breaking sea waves by high resolution radar IKI-2M

Wykrywanie zjawiska załamania się fal za pomocą radaru wysokiej rozdzielczości IKI-2M

Yu. Kravtsov[1], M.D. Raev[2], E.I. Skvortsov[2]

[1] Institute of Mathematics Physics and Chemistry, Maritime University of Szczecin, Poland
[2] Space Research Institute, Moscow, Russia

Key words: sea radars, breaking waves

Abstract
Two polarization mobile X-band radar IKI-2M, developed by Space Research Institute, Russ. Acad. Sci., has sufficiently high resolution of order 5–7 m both in distance and in azimuthally direction and is able to study sufficiently small details of the sea surface. This paper outlines the results of the sea surface observations, performed in 2008 in Gelendzhik, the Black Sea, at low grazing angles. Using radar images of the sea surface, presented in "time-distance" format, two kinds of wave breaking were observed: traditional "macro-breakings", answering to long gravity waves, and "micro-breakings", which correspond to small-scale breaking waves of meso-scale (decimeter) range, which never were registered by radar so far. These two kinds of wave-breakings differ by their intensities, velocities of movement, life-times and polarization characteristic. "Macro-breakings" are produced by long gravity waves with velocities, exceeding 5–8 m/s. They demonstrate rather long life-times about 10–20 s and sufficiently high radar cross-section up to 5–10 m^2. In distinction to the "macro-breakings", the "micro-breakings" are generated by slow meso-waves with velocities about 0.5–2.5 m/s. They do not produce the foam, have short life-time about 2–3 s and sometimes demonstrate very high radar cross-section up to several m^2. Both types of breaking waves may produce significant clatter for marine radar and should be taken into account in solution of problems, connected with the safety of navigation and shipping.

Słowa kluczowe: radary morskie, fale załamujące się

Abstrakt
Przenośny radar IKI-2M z podwójną polaryzacją, opracowany przez Instytut Badań Kosmicznych Russ. Acad. Sci., posiada rozdzielczość rzędu 5–7 m zarówno w odległości, jak i w kierunku azymutalnym, by być w stanie przebadać szczegóły powierzchni morza. W artykule przedstawiono wyniki obserwacji powierzchni morza, przeprowadzone w 2008 roku w Gelendzhik na Morzu Czarnym, przy niskich kątach padania. Przy użyciu obrazów radarowych powierzchni morza, przedstawionych w formacie czas – odległość, zaobserwowano dwa rodzaje załamań fal: tradycyjne „makrozałamujące się", odpowiadające falom długim grawitacyjnym oraz „mikrozałamujące się", które odpowiadają małym załamującym się mezofalom (decymetrowe), które nie zostały nigdy zarejestrowane przez radar. Te dwa rodzaje załamujących się fal różnią się intensywnością, prędkościami ruchu, czasem trwania oraz charakterystyką polaryzacji. Fale „makrozałamujące się" są tworzone przez długie fale grawitacyjne, uzyskują prędkość powyżej 5–8 m/s. Charakteryzują się raczej długim czasem trwania, ok. 10–20 sekund oraz wystarczająco wysokim przekrojem radarowym do 5–10 m^2. W odróżnieniu do fal „makrozałamujących się", fale „mikrozałamujące się" są tworzone przez małe mezofale o prędkości ok. 0,5–2,5 m/s. Nie tworzą one piany, charakteryzują się krótkim czasem trwania ok. 2–3 sekund i wykazują bardzo wysoki przekrój radarowy, do kilku m^2. Oba typy załamujących się fal mogą tworzyć znaczące szumy na ekranach radarów morskich i powinny zostać wzięte pod uwagę w rozwiązywaniu problemów dotyczących bezpieczeństwa nawigacji i żeglugi.

Introduction

Time-distance regime in radar measurements is realized by fixing antenna's azimuthal angle and registering intensity $I_n(x)$ of the echo signal for every pulse, emitted at discrete time-moments $\tau_n = nT$, $n = 1,2\ldots$. Here T is time interval between pulses and x is a distance from radar antenna. Presenting the measured intensity $I_n(x)$ on time-distance plane (x,τ) and considering $\tau = nT$ as continuous variable, we may study the "tracks", formed on the (x,τ) plane by targets and wave processes.

In the case of point target, moving to antenna with radial velocity v within the main lobe of directivity pattern, echo signal is concentrated near target trajectory $x(\tau)$, which is seen as track $x(\tau)$ on the (x,τ) plane. Uniformly moving target forms straight line trajectory:

$$x = x_0 - v(\tau - \tau_0) \tag{1}$$

where x_0 is an initial target position at $\tau = \tau_0$.

The long gravity waves on the sea surface manifest themselves by small-scale ripples, which scatter radar signal. The surface wave, uniformly moving to antenna with phase velocity v_{ph}, produces on the (x,τ) plane the rectilinear track.

$$x = x_0 - v_{ph}(\tau - \tau_0) \tag{2}$$

This track, presented by continuous straight line a) on figure 1, is quite similar to the track of the uniformly moving point target, eq. (1).

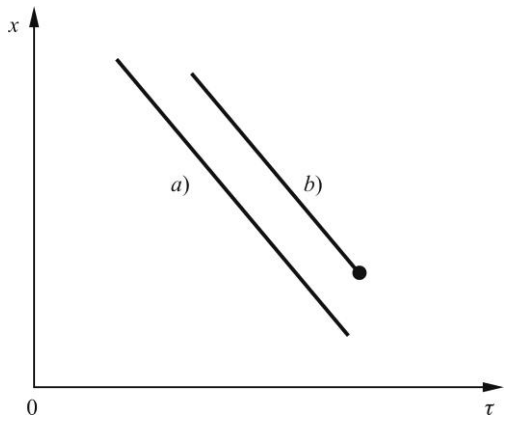

Fig. 1. Rectilinear tracks on the time-distance plane (x,τ): a) continuous track, corresponding to uniformly moving gravity wave; b) – finite track, corresponding to the breaking gravity wave ("macro-breaking" phenomenon)

Rys. 1. Prostoliniowe trasy na wykresie zależności odległości od czasu (x,τ): a) ciągła trasa, odpowiadająca poruszającej się jednostajnie fali grawitacyjnej; b) trasa określona, odpowiadająca załamującej się fali grawitacyjnej (zjawisko „makrozałamywania się")

Observing rectilinear tracks of long gravity waves and making use of dispersion relation:

$$v_{ph}^2 = g / k \tag{3}$$

connecting the phase velocity $v_{ph} = \omega/k$ of the long gravity waves with frequency ω, wave number k and gravity constant $g = 9.8$ m/s^2, one can estimate dominating wavelength

$$\lambda_{dom} = \frac{2\pi}{k} = \frac{2\pi}{g} v_{ph}^2 \tag{4}$$

and thereby distinguish the wave packets of different wavelengths.

The tracks, produced by gravity waves on (x,τ) plane, were studied in [1, 2] for revealing the nonlinear interaction of gravity waves, in particular, for detecting the second harmonics of dominating, i.e. energy bearing waves. The same technique was used in [3] for detection of so called "return waves", propagating against the wind and arising due to nonlinear interaction between the swell of narrow angle spectrum and wind waves of wide spectrum.

In this paper we use time-distance regime for registration of the breaking waves on the sea surface. Breaking waves manifest themselves by characteristic sharp-ended tracks on the (x,τ) plane, schematically shown by the finite curve b) at the figure 1. Observations of finite tracks have revealed two kinds of breaking waves: "macro-breakings" and "micro-breakings", which will be described below.

Observations of finite tracks, corresponding to macro- and micro-breakings

Two polarization high resolution radar IKI-2M was developed by the Space Research Institute of the Russian Academy of Sciences for detailed studying the wave processes on the sea surface. Radar has a wavelength 3 cm, X-band. Pulse duration $T_p = 40$ ns provides radial resolution $\Delta x \approx 6$ m. The width of directivity pattern $\Delta\varphi = 1°$ corresponds to azimuthally resolution about 7.5 m at a distance 1 km.

Radar IKI-2M was installed on the roof of the container laboratory on the height 10 m over water surface (see photo fig. 2).

In turn the laboratory container was placed in the end of the long, about 200 m length, mole in the Blue Bay near Gelendzhik (Novorossiysk district, North shore of the Black Sea). Antenna was oriented in the South direction, oppositely to waves, moving mainly to the North.

Radar images of the sea surface, registered in the time-distance regime, have revealed the finite tracks of two kinds. The tracks of the first kind move to radar with velocity 6–8 m/s, characteristic for gravity waves of wavelength 10–20 m. At the moment of breaking, the gravity wave gives rise to turbulent water flow, described as the "boiling water state". This kind of wave breaking we identify with the phenomenon of "macro-breaking".

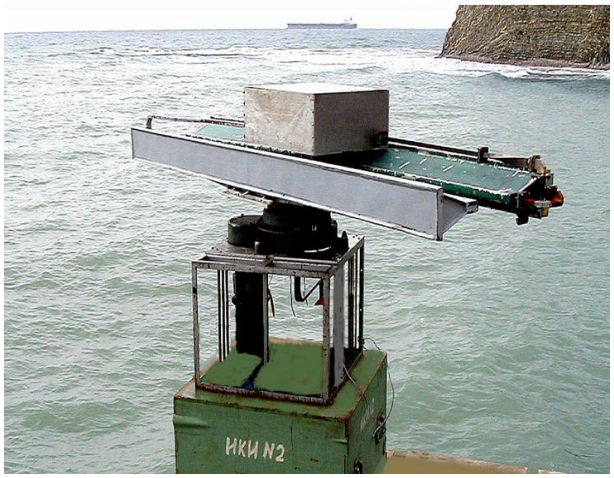

Fig. 2. Radar IKI-2M, installed on the roof of the container laboratory in the Blue Bay, near Gelendzhik, the Black Sea
Rys. 2. Radar IKI-2M, zainstalowany na szczycie kontenera – laboratorium w Blue Bay, niedaleko Gelendzhik, Morze Czarne

General picture of tracks, seen at the radar display at vertical polarization, is presented at figure 3, which embraces time-interval 125 s and distances 320–900 m. Two tracks, answering to the phenomenon of "macro-breaking", are selected by signatures. Typical duration of the bright part of the track is about 2–10 s, whereas duration of the whole track might be few tens or few hundreds seconds. This duration is comparable with the time of the wave being within directivity pattern.

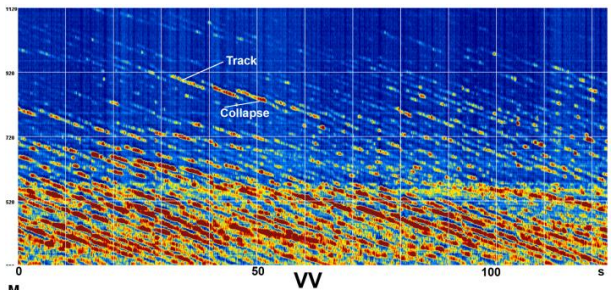

Fig. 3. Tracks on the time-distance plane (x,τ), corresponding to gravity waves, moving with the velocity 6–8 m/s
Rys. 3. Trasy odpowiadające falom grawitacyjnym, poruszające się z prędkością 6–8 m/s

Besides macro-breakings, our experiments of 2008 have revealed "micro-breakings", which manifest themselves as series of short finite tracks, which duration is less, than 1 s, shown at figure 4 for horizontal polarization. Typical velocity of the sea waves, experiencing micro-breaking, is estimated as 0.4–0.6 m/s.

It is reasonable to identify "micro-breakings" with the surface waves of meso-scale (decimeter) spectrum. They are regarded here as "meso-waves", because their characteristic length 30–60 cm happens to be intermediate between capillary-gravity waves of 1–3 cm length and long gravity waves with wavelength of few meters and longer. Mesowaves arise eventually due to small scale instabilities of the water surface near crest of long gravity waves. As was pointed out in [4, 5, 6, 7, 8], the phenomenon of micro-breakings may play an important role in forming SAR images of the sea surface. Figure 4 presents as the first radar observation of mesowaves from small distances. Along with radar observations of mesowaves' fine structure, the experiments of 2008 have registered also the optical images of mesowaves, which are shown at figure 5.

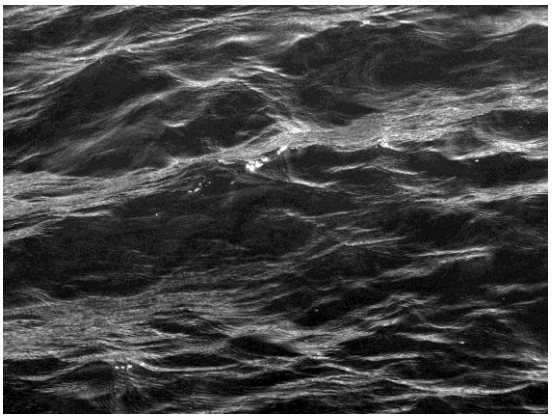

Fig. 4. Micro-breaking phenomenon, observed on the (x, τ) plane in the form of series of short tracks of duration no more than 1 s. Typical velocity of breaking meso-waves is as low as 0.4–0.6 m/s
Rys. 4. Zjawisko „mikrozałamywania się", obserwowane w formie serii krótkich tras o czasie trwania nie większym niż 1 s. Typowa prędkość załamujących się mezofal jest mniejsza od 0,4–0,6 m

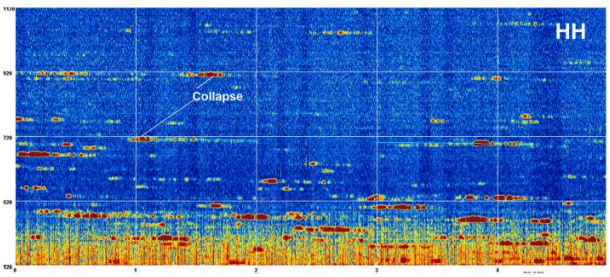

Fig. 5. Photo image of meso-waves, experiencing "micro--breaking"
Rys. 5. Zdjęcie mezofal podczas mikrozałamywania

It is worth noticing that meso-waves break up comparatively quickly after their arising, so that the tracks, corresponding to micro-breakings, are seen no more than 1–2 s.

In what follows we describe some properties of the macro- and micro-breakings.

Coherent and incoherent components of the signal, scattered by macro-breakings

Microwave scattering from very irregular water--air mix, raised after macro-breakings, is of incoherent nature, because the scattering elements of the turbulent mix take random positions relatively their neighbors. Such a backscattering can not be described by the Bragg (resonant) mechanism of scattering, because of the height of inhomogeneities of the water surface is significantly larger as compared with the radar wavelength.

It seems naturally to assume the resulting cross--section to be proportional to the visible area S_{vis} of the water-air turbulent mix:

$$\sigma_{tot} = \chi S_{vis}, \quad \chi \le 1 \tag{5}$$

where χ is an averaged reflectivity factor.

This intuitively acceptable phenomenological relation can be illustrated by following qualitative model of scattering. Let the water-air mix consists of randomly positioned water spheres of radius ρ. Because of high conductivity of the sea water in microwave band, we may ascribe cross-section $\sigma_1 = \pi\rho^2$ to every water sphere, similar to metallic sphere. Then total radar cross-section of the turbulent water-air mix is determined by the number N of scattering spheres on the sea surface, which can be estimated as $N = S_{vis}/\pi\rho^2$. It leads to the relation

$$\sigma_{tot} = N\sigma_1 \approx \sigma_1 S_{vis}/\pi\rho^2 \approx S_{vis} \tag{6}$$

which is a partial case of eq. (5) for $\chi = 1$.

Proportionality between total cross-section σ_{tot} and visible surface S_{vis} can be derived also for scattering elements of non-spherical form and for elements, obeying statistical distribution. Coefficient of proportionality χ in (5) depends mainly on microwave absorption in the air bubbles. Due to stochastic nature of the turbulent water surface, one may think that the coefficient of proportionality χ in (5) only weakly depends on the radar wavelength, on the angle of incidence and on polarization of the incident wave.

The visual surface S_{vis} of the macro-breaking can be estimated as 10–20 m^2. Based on phenomenological relation (5), the radar cross-section σ_{tot} of the macro-breaking also can be estimate by 10–20 m^2. Such a cross-section causes bright spot in the end of wave track, which visually looks as much as 10–20 times brighter than continuous track, formed by ripples on the crest of gravity wave due to Bragg mechanism of scattering.

Though incoherent scattering dominates, some elements of macro-breakings may demonstrate the features of coherent scattering. First of all it concerns sharp-ended water wedges, which might be formed, at low wind velocity, just before wave's breaking. If L is the length of the rectilinear wedge, the coherent cross-section is estimated as $S_{coh} \approx L\lambda$, because only λ – vicinity of the water wedge forms the scattered wave. As a result, the coherent component of radar cross-section will be:

$$\sigma_{coh} \approx \frac{S_{coh}^2}{\lambda^2} \approx L^2 \tag{7}$$

Thus, rectilinear wedge of 1 m length might give rise to the coherent cross-section of order 1 m^2, comparable with cross-section of small boat.

The other elements, which may contribute into coherent cross-section, are smooth water flows (water films), sometimes arising in the front of macro-breakings. Let R_1 and R_2 are curvature radii of the smooth water film, visible by radar. Then $S_{coh} \approx \pi R_1 R_2$ and

$$\sigma_{coh} \approx \frac{S_{coh}^2}{\lambda^2} \approx \frac{\pi R_1^2 R_2^2}{\lambda^2} \tag{8}$$

For $R_1 \sim R_2 \sim 0.2$ m and $\lambda = 3$ cm this cross--section may take gigantic value about $\sigma_{coh} \sim 16$ m^2, comparable with in coherent cross-section of motor or patrol boat.

Backscattering from micro-breakings

Though the waves of meso-scale spectrum, responsible for micro-breakings, have comparatively small height about 15–20 cm, they may cause rather strong echo signal. There are two reasons which increase backscattering. The first one is sharp-crested form of mesowaves just before breaking. The coherent component of radar cross--section, brought about by the sharp-ended crest, is described by eq. (7). Similarly to macro-breakings, the radar cross-section might be as large as 1 m^2.

The second factor is the phenomenon of multiple diffractions due to concave shape of the breaking meso-wave (fig. 6). The phenomenon of multiple diffractions can be described in the framework of the geometrical theory of diffraction [4, 5, 6, 7, 8, 9].

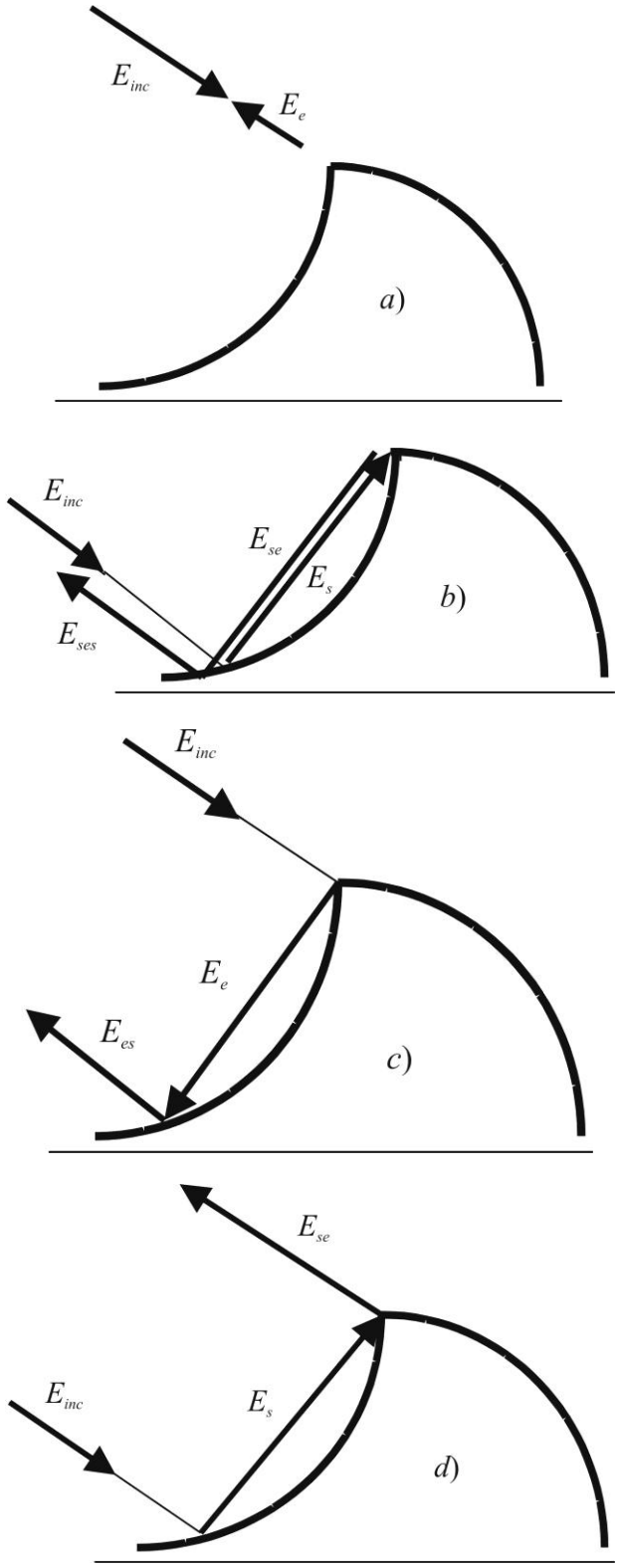

Fig. 6. The four-channel model of backscattering from the sharp-crested meso-waves: a) single scattering, answering to the edge wave E_e; b) triple scattering, producing the wave E_{ses}; c) and d)double scattering, producing a pair of the coherent wave fields E_{es} and E_{se}

Rys. 6. Czterokanałowy model wstecznego rozpraszania dla fal o ostrych grzbietach: a) pojedyncze rozpraszanie, odpowiadające brzegowi fali E_e, b) potrójne rozpraszanie, tworzące falę E_{ses}, c) i d) podwójne rozpraszanie, tworzące parę koherentnych pół falowych E_{es} i E_{se}

The incident wave excites, first of all, the "edge" wave E_e (fig. 6a), which diverges from the sharp crest of the water wedge. The edge wave E_e in turn brings about the waves E_{es}, E_{ess}, E_{esss} and so on, multiply reflecting from the wedge footnote (figure 6c shows only first-order wave E_{es}). The primary electromagnetic wave, incident on a concave front side of a meso-wave, may produce also specularly reflected wave E_s, E_{ss}, E_{sss}, ..., as well as the edge wave E_{se} (fig. 6d) and its byproducts E_{ses}, E_{sess}, …. Every term among the listed wave fields can be treated as a channel of multiple diffractions, as it was presented in the papers [4, 5, 6, 7, 8, 9].

The most important features of multiple diffractions at curvilinear wedge are presented by the "four channel model," which includes the following four terms:

$$E_{scat} = E_e + E_{es} + E_{se} + E_{ses} \tag{9}$$

The first term is an edge wave, mentioned above (fig. 6a). This wave returns to the radar antenna after the single act of diffraction at the curvilinear wedge crest. The second term E_{es}, excited by the edge wave, returns to the radar antenna after specular reflection from the wedge foot (fig. 6c). The third term E_{se} is a wave, which firstly is reflected from the wedge foot and then diffracted at the wedge sharp crest (fig. 6d). In virtue of reciprocity theorem double diffracted wave fields E_{es} and E_{se} are coherent to each other:

$$E_{es} = E_{se} \tag{10}$$

These two terms are responsible for the enhanced backscattering phenomenon, caused by multi-path (or multi-channel) scattering. The fourth term in eq. (9) corresponds to triple diffraction: first specular reflection occurs from the wedge foot, which is followed with a diffraction by the sharp crest and at last with the second reflection from the wedge (fig. 6b).

In frame of the "four channel" model (9) an intensity of the scattered wave field is given by the equation

$$I_{scat} = I_e + 4I_{es} + I_{ses} \sim 6I_e \tag{11}$$

where it is accounted that the channels E_{es} and E_{se} are coherent to each other according to eq. (10), while the other channels are mutually incoherent. Thus, multiple diffractions are responsible for the phenomenon of the enhanced backscattering. According to eq. (11) the phenomenon of the enhanced backscattering increases cross-section a few times as compared with the single channel.

The enhanced backscattering phenomenon is important mainly for horizontal polarization, because the signal of vertical polarization is undergoing to serious damping due to Brewster phenomenon [9]. Brewster damping makes radar images of meso-waves at vertical and horizontal polarization quite different, as it was emphasized still in [8].

Conclusions

The experiments, performed in the Blue Bay in 2008, have revealed two kinds of the breaking waves, contributing into radar images of the sea surface. It is shown that the radar cross-section of macro- and micro-breakings might be sufficiently large, so that they can be accepted for false targets on the sea surface. The echo signals from micro--breakings at most a few seconds, whereas the reflections from macro-breakings continue up to 10 s. In these conditions the effective method for distinguishing the breaking waves from the real objects might be correlation processing. We hope that obtained results will be helpful for secure navigation and shipping in the coastal zone.

References

1. BULATOV M.G., RAEV M.D., SKVORTSOV E.I.: Radar observations of the nonlinear wave processes in the coastal zone. The Third All-Russia Open Conference "Modern problems of the remote sensing of the Earth from the space. Moscow, the Space Research Institute of the Russian Academy of Sciences, 14–17 November 2005, Proceedings, 50–55.
2. BULATOV M.G., RAEV M.D., SKVORTSOV E.I.: Study of nonlinear waves on the basis of the spatial-frequency spectra of the radar images of the sea surface. The Earth Studies from the Space. 2006. №2, 64–70.
3. BULATOV M.G., RAEV M.D., SKVORTSOV E.I.: Return waves on the sea surface. Physics of Wave Phenomena (Allerton Press, Inc.), 2008,16 (1), 70–75.
4. KRAVTSOV YU.A., MITYAGINA M.I., CHURYUMOV A.N.: Non-resonant mechanism of electromagnetic waves scattering by sea surface: scattering by the steep sharpened waves, Radio Phys. Quant. Electron., 1999, 42 (3), 216–228.
5. KRAVTSOV YU.A., MITYAGINA M.I., CHURYUMOV A.N.: Electromagnetic waves backscattering by meso-scale breaking waves on the sea surface, Bull. Russ. Acad. Sci., Ser. Physics, 1999, 63 (12), 1859–1865.
6. CHURYUMOV A.N., KRAVTSOV YU.A.: Microwave backscatter from mesoscale breaking waves on the sea surface, Waves in. Random Media, 2000, 10 (1), 1–15.
7. CHURYUMOV A.N., KRAVTSOV YU.A., LAVROVA O.YU., LITOVCHENKO K.TS., MITYAGINA M.I., SABININ K.D.: Signatures of resonant and non-resonant scattering mechanisms on radar images of the internal waves. Int. J. Remote Sens. 2002, 23 (20), 4341–4355.
8. BULATOV M.G., KRAVTSOV YU.A., LAVROVA O.YU., LITOVCHENKO K.TS., MITIAGINA M.I., RAEV M.D., SABININ K.D., TROKHIMOVSKII YU.G., CHURIUMOV A.N., SHUGAN I.V.: Physical mechanisms of aerospace radar imaging of the ocean, Physics-Uspekhi, 2003, 46 (1), 63–79.
9. KRAVTSOV YU.A., ZHU NING YAN: Multiple diffractions of electromagnetic waves by a wedge of concave shape. Wave Motion, 2006, 43, 206–221.

Recenzent:
prof. dr hab. inż. Bolesław Mazurkiewicz
Akademia Morska w Szczecinie